Robustness Analysis of An Structure Dependent Explicit Integration Algorithm for Real-Time Structural Testing

Cheng Chen, Julie Leong and Olga Mendez
School of Engineering, San Francisco State University, San Francisco, CA 94132

ABSTRACT:
Real-time testing provides a viable experiment technique for performance evaluation of structures with rate-dependent devices. Explicit integration algorithms are usually preferred over implicit algorithms in real-time testing since no iterations are required. Conditional stability of conventional explicit algorithms however has significantly restricted their application in real-time structural testing. Recently, an unconditionally stable explicit integration algorithm has been developed and successfully implemented for real-time testing. An important property of this explicit algorithm is the dependence of its integration parameters on properties of the structure to be solved. This brings concern when applying this algorithm in real-time testing since the structural properties might not be accurately known before the tests or vary during the tests. This paper presents an robustness analysis of the effect of estimated structural properties on the stability and accuracy of this algorithm for real-time testing. Numerical simulations of structures are conducted to demonstrate the effectiveness of presented study.

Keywords: real-time, integration algorithm, robustness, stability, accuracy

1. INTRODUCTION

Structural testing is important for earthquake engineering research when the structure or its components are difficult to model. Different testing methods have been developed by researchers, such as quasi-static testing method, pseudodynamic testing method, hybrid (substructure) testing method and shake table testing method. Application of these testing methods has significantly contributed to structural engineering research [Oliva *et al.* 1990; Zhang and Ricles 2006; Fahnestock *et al.* 2007]. For quasi-static testing and shake table testing methods, the command displacement for the servo-hydraulic actuators are usually predefined based on the user-defined loading protocol or selected ground motion; while for pseudodynamic testing and hybrid testing methods the command displacements are computed on-line by solving the equations of motion of the prototype structure using a numerical integration algorithm. The stability and accuracy of the integration algorithm are therefore vital for a stable and reliable pseudodynamic/hybrid test. Analysis of integration algorithms for pseudodynamic testing has been conducted by researchers [Shing and Vannan 1991; Shing *et al.* 1991]. Recently, innovative energy dissipation devices have been investigated by researchers to improve seismic performances of civil engineering structures, such as the magneto-rheological (MR) dampers [Yang *et al.* 2002]. To realistically evaluate these devices requires the structural tests to be conducted at a real-time scale. The pseudodynamic testing and hybrid testing methods are therefore extended to real-time scale, i.e., real-time pseudodynamic testing and real-time hybrid testing methods, which will be referred to as real-time testing methods in this paper.

Unlike the conventional pseudodynamic and hybrid testing methods, the command displacements in a real-time test are imposed at a real-time scale by servo-hydraulic actuator(s) to the experimental structure(s) and therefore have to be available at the beginning of each integration time step. This renders the explicit integration algorithms to be preferred over the implicit algorithms in real-time

testing. However, the commonly used explicit integration algorithms such as the central difference method and the Newmark explicit method are only conditionally stable and therefore have a restriction on the time step size due to numerical stability. When the total number of degrees of freedom of the structural system becomes large, high natural frequencies can exist and controls the time step size for stability. An extremely small time step value will make the implement of the integration algorithm difficult for real-time testing using the state-of-the-art servo-hydraulic equipment. Implicit integration algorithms however are usually unconditionally stable and have also been investigated for real-time testing [Shing 2002; Chen and Ricles 2011]. Implementation of an implicit algorithm however involves larger amount of computation when compared with explicit integration algorithms.

To advance the application of real-time testing for structural engineering research, a new unconditionally stable explicit integration algorithm was developed by Chen and Ricles [2008a]. By applying the discrete control theory, the explicit CR algorithm is shown to be unconditionally stable for linear elastic structures and nonlinear structures with softening behavior when the linear elastic structural properties are used for the integration parameters [Chen and Ricles 2008b]. The characteristics of explicitness and unconditional stability make the CR integration algorithm appealing for conventional pseudodynamic testing as well as for real-time testing. Lin *et al.* [2008] applied the explicit CR integration algorithm to the pseudodynamic testing of a four-story four-bay self-centering moment resisting frame. A static test was conducted to estimate the stiffness matrix of the experimental structure. The experimental results are shown to have a good comparison with the numerical analysis using OpenSees [Seo *et al.* 2008]. Chen *et al.* [2009] applied the CR algorithm in real-time hybrid tests of moment resisting frame with an elastomeric damper. The equivalent damping and stiffness of the rate-dependent elastomeric damper near the first natural frequency of the structure was accounted for in the integration parameters. The experimental results were compared with that using the HHT α-method with a fixed number of substep iterations and good agreement was observed.

An important property of the explicit CR algorithm is that its integration parameters are dependent on the structural properties instead of being constants. This requires estimating the properties of experimental structure before the tests. Since the mass and inherent viscous damping are usually analytically defined in a pseudodynamic or hybrid test, it is reasonable to assume that their accurate values are used in real-time tests. However, the restoring force related structural stiffness may not be estimated easily and accurately. Moreover, when the real-time testing method is used to simulate the structural response to an earthquake, the experimental structure may develop nonlinearity during the test, leading to stiffness degradation. This poses challenges to the application of CR algorithm for real-time testing and requires a systematic analysis of the influence of estimated structural stiffness on the CR algorithm in real-time testing for structural research. This present study serves this objective through numerical analysis of the explicit CR algorithm for real-time testing when estimated structural properties are used.

2. Unconditionally Stable Explicit CR Integration Algorithm

A single degree-of-freedom (SDOF) system subjected to an excitation $F(t)$ as shown in Fig. 2.1 is used for the analysis in this paper. The differential equation of motion can be written as

$$m \cdot \ddot{x}(t) + c \cdot \dot{x}(t) + r(t) = F(t) \tag{2.1}$$

where m and c are the mass and inherent viscous damping of the SDOF system, respectively; and $r(t)$ is the restoring force of the spring. When the spring is linear elastic, the restoring force can be calculated as $r(t) = k \cdot x(t)$, where k is the linear elastic stiffness of the spring and $x(t)$ is the displacement response of the SDOF system. The natural frequency and damping ratio of the SDOF system can be determined as $\omega_n = \sqrt{k/m}$ and $\zeta_n = \sqrt{c/(2m\omega_n)}$. For real-time testing, a numerical integration algorithm is used to solve the temporally discretized equation of motion as follows

$$m \cdot \ddot{x}_{i+1} + c \cdot \dot{x}_{i+1} + r_{i+1} = F_{i+1} \tag{2.2}$$

In Eq. (2.2) $\dot{x}_{i+1}$ and $\ddot{x}_{i+1}$ are the velocity and acceleration of the SDOF system at the $(i+1)^{th}$ time step, respectively; r_{i+1} and F_{i+1} are the restoring force of the spring and the external excitation at the $(i+1)^{th}$ time step, respectively.
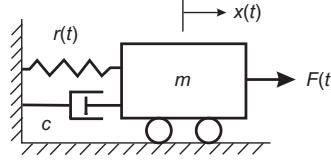

Figure 2.1 Schematic of real-time pseudodynamic testing of a SDOF system

The variation of displacement and velocity over the time step for the explicit CR integration algorithm [Chen and Ricles 2008a] are defined as

$$\dot{x}_{i+1} = \dot{x}_i + \alpha_1 \cdot \Delta t \cdot \ddot{x}_i \tag{2.3a}$$

$$x_{i+1} = x_i + \Delta t \cdot \dot{x}_i + \alpha_2 \cdot \Delta t^2 \cdot \ddot{x}_i \tag{2.3b}$$

where Δt is the integration time step; x_i and x_{i+1} are the displacement response of the SDOF system at the ith and $(i+1)^{th}$ time step, respectively; α_1 and α_2 are integration parameters. To attain unconditional stability for linear elastic structures, the integration parameters in Eqs. (2.3a) and (2.3b) are defined as:

$$\alpha_1 = \alpha_2 = \frac{4m}{4m + 2c \cdot \Delta t + k \cdot \Delta t^2} \tag{2.4}$$

The CR algorithm can be observed to be explicit for both displacement and velocity, which makes the algorithm appealing for real-time testing. However, it can also be observed that accurate information of the structural properties (m, c, and k) is required for the parameters to achieve unconditional stability for linear elastic structures. This poses challenges for researchers when applying the CR algorithm for real-time testing since the stiffness may not be identified accurately for an experimental structure and this structural stiffness might also vary due to nonlinearity during a real-time test. This present study focuses on the effect of estimated stiffness on the stability and accuracy of the explicit CR algorithm using a discrete transfer function approach.

For a linear elastic structure in Eq. (2.2), Chen and Ricles [2008a] showed that the CR algorithm can be represented by a discrete transfer function expressed in the following general form

$$G(z) = \frac{X(z)}{F(z)} = \frac{n_2 \cdot z^2 + n_1 \cdot z + n_0}{d_2 \cdot z^2 + d_1 \cdot z + d_0} \tag{2.5}$$

where $X(z)$ and $F(z)$ are discrete z-transforms of the displacement x_i and excitation force F_i, respectively; n_i and d_i ($i=0$ to 2) are coefficients of the numerator and denominator, and are tabulated in Table 2.1. The solution for z in the complex z-domain that renders the denominator of $G(z)$ in Eq. (2.5) to be zero is defined as a "pole" of the discrete transfer function [Ogata 1995]. The denominator of the discrete transfer function is also the characteristic equation of the integration algorithm. The stability of a discrete transfer function is determined by its poles. If the discrete function in Eq. (2.5) has all of its poles located inside, or on the unit circle in the complex z-domain the discrete system is stable. Otherwise it is unstable.

3. STABILITY ANALYSIS OF CR INTEGRATION ALGORITHM UNDER ESTIMATED STIFFNESS

When an estimated stiffness k_{es}, instead of the actual stiffness k, is used for the explicit CR algorithm, the integration parameters in Eqs. (2.3a) and (2.3b) are modified as

$$\alpha_1 = \alpha_2 = \frac{4m}{4m + 4c \cdot \Delta t + k_{es} \cdot \Delta t^2} \tag{3.1}$$

The discrete transfer function for the *CR* algorithm with integration parameters in Eq. (3.1) can be derived and expressed in the general form of Eq. (2.5). The coefficients of the resulting discrete transfer function are tabulated in Tables 3.1, which can be demonstrated to be same as those in Tables 2.1 when the estimated stiffness is equal to the actual stiffness.

Table 3.1. Coefficients of $G(z)$ for CR algorithm with estimated stiffness

Numerator		Denominator	
n_2	0	d_2	$4m + 2 \cdot c \cdot \Delta t + k_{es} \cdot \Delta t^2$
n_1	$4\Delta t^2$	d_1	$-8m - 2k_{es} \cdot \Delta t^2 + 4k \cdot \Delta t^2$
n_0	0	d_0	$4m - 2 \cdot c \cdot \Delta t + k_{es} \cdot \Delta t^2$

The characteristic equation of the *CR* algorithm with estimated stiffness can be derived as

$$(4m + 2c\Delta t + k_{es}\Delta t^2) \cdot z^2 + (-8m - 2k_{es}\Delta t^2 + 4k\Delta t^2) \cdot z + (4m - 2c\Delta t + k_{es}\Delta t^2) = 0 \tag{3.2a}$$

For given invariant structural properties (m, c and k) and variable estimated stiffness k_{es}, the critical value of estimated stiffness (k_{es}) for stable poles of Eq. (3.2a) can be derived using the root locus approach from discrete control theory [Ogata 1995; Franklin *et al.* 2002], where Eq. (3.2a) can be rewritten as

$$1 + \frac{(z^2 - 2z + 1) \cdot \Delta t^2}{(4m + 2c\Delta t) \cdot z^2 - (8m - 4k\Delta t^2) \cdot z + (4m - 2c\Delta t)} \cdot k_{es} = 0 \tag{3.2b}$$

For varying values of k_{es}, the location for the solution of z in the discrete domain can be derived by plotting the root locus of the following discrete transfer function

$$G_o(z) = \frac{(z^2 - 2z + 1) \cdot \Delta t^2}{(4m + 2c\Delta t) \cdot z^2 - (8m - 4k\Delta t^2) \cdot z + (4m - 2c\Delta t)} \tag{3.3}$$
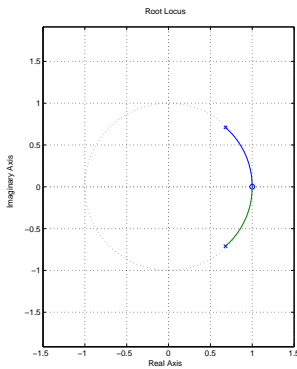

Figure 3.1. Typical root loci for $G_o(z)$ of CR algorithm with estimated stiffness
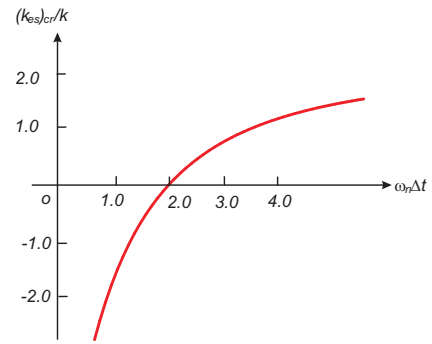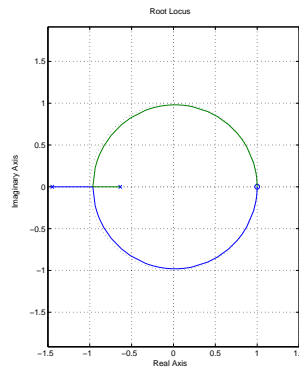
Figure 3.2. Stable regions of estimated stiffness k_{es} and $\omega_n \Delta t$ for CR algorithm

The discrete transfer function in Eq. (3.3) can be observed to have duplicate zeros of z=1, which are independent of structural properties, and two poles, which are dependent on the structural properties (m, c, k) and integration time step (Δt). The root loci of the discrete transfer function in Eq. (3.3) have two branches. As the value of the estimated stiffness k_{es} in Eq. (3.2b) increases from zero to infinity, the root loci of $G_o(z)$ starts at the poles of the transfer function in Eq. (3.3) and terminates at its zeros. If the root locus falls on or within the unit circle, the characteristic equation in Eq. (3.2a) then has stable poles, implying that the CR algorithm will be stable for all possible positive values of estimated stiffness. Otherwise, unstable poles exist for the characteristic equation in Eq. (3.2a) and the algorithm is only stable for selected range of positive values of the estimated stiffness.

Fig. 3.1 shows typical root loci of the open loop transfer function $G_o(z)$ in Eq. (3.3) with ζ_n=0.02, Δt=0.01 $sec.$ and different natural frequencies of ω_n=$\pi/4$ and ω_n=$13\pi/2$ in Figs. 3.1(a) and 3.1(b), respectively. For a smaller value of ω_n (i.e., ω_n=$\pi/4$), both branches of the root loci in Fig. 3.1(a) are located in the unit circle of the discrete z-domain, which means that the characteristic equation in Eq. (3.2a) will always have stable poles for any non-negative value of the estimated stiffness. The stability of the CR algorithm in this case is therefore not affected by using the estimated stiffness for the integration parameters. For the larger value of ω_n (i.e., ω_n=$13\pi/2$), the transfer function in Eq. (3.3) has one pole located outside the unit circle. Based on the definition of root locus approach in control theory, part of the root loci outside the unit circle as shown in Fig. 3.1(b) will lead to unstable poles for the characteristic equation in Eq. (3.2a) and thus unstable CR algorithm. This indicates that the CR algorithm for a large value of ω_n is stable for a selected range of estimated stiffness.

It can also be observed from Fig. 3.1(b) that the critical value of k_{es}, if instability exists, always occurs when the root locus crosses the point of z=-1 in the discrete z-domain. The critical value of k_{es} therefore can be determined by substituting z=-1 into Eq. (3.2a), which leads to

$$16m + 4(k_{es})_{cr}\Delta t^2 - 4k\Delta t^2 = 0 \tag{3.4}$$

Eq. (3.4) can be rewritten as

$$\frac{(k_{es})_{cr}}{k} = 1 - \frac{4}{\omega_n^2 \Delta t^2} \tag{3.5a}$$

Eq. (3.5a) gives the critical value of estimated stiffness to achieve a stable CR algorithm when an estimated stiffness is used to determine the integration parameters. Combined with the observation from the root locus presented in Fig. 3.1, the stable region of k_{es} can be determined as $k_{es} \geq (k_{es})_{cr}$. Eq. (3.5a) also indicates that the critical value of $(k_{es})_{cr}$ for CR algorithm is independent of the inherent viscous damping of the structure. For small values of $\omega_n\Delta t$, Eq. (3.5a) gives a negative value of $(k_{es})_{cr}$, which means that the CR algorithm will be always stable for any positive value of estimated stiffness k_{es}, which is consistent with the observation from Fig. 3.1(a). When the value of $\omega_n\Delta t$ becomes larger, Eq. (3.5a) gives a positive value of $(k_{es})_{cr}$. In this case the CR algorithm would be stable only when the estimated stiffness k_{es} is larger than $(k_{es})_{cr}$ (corresponding to Fig. 3.1(b)). The stable limit of k_{es}/k for the CR algorithm is presented in Fig. 3.2 for different values of $\omega_n\Delta t$.

Eq. (3.4) can also be written as following to give the critical value of $(\omega_n\Delta t)_{cr}$ for a selected value of k_{es},

$$(\omega_n\Delta t)_{cr}^2 = \frac{4}{1 - k_{es}/k} \tag{3.5b}$$

For a ratio of k_{es}/k smaller than 1.0 (i.e. an underestimation of the experiment structure stiffness), Eq. (3.5b) gives a positive real solution of $\omega_n\Delta t$. The CR algorithm is stable for any value of $\omega_n\Delta t \leq (\omega_n\Delta t)_{cr}$.

When the value of k_{es}/k is greater than or equal to 1.0, Eq. (3.5b) does not have a real solution. The CR algorithm is therefore stable for any value of $\omega_n \Delta t$. When the estimated stiffness is equal to zero, i.e., $k_{es}/k = 0$, Eq. (3.5b) gives the stability region of $\omega_n \Delta t \leq 2.0$, which is same as the stability limit for the Newmark Explicit Method [Newmark 1959].

4. ACCURACY ANALYSIS OF CR ALGORITHM UNDER ESTIMATED STIFFNESS

The two poles of the discrete transfer function for the CR algorithm can be written as

$$p_{1,2} = \sigma \pm \varepsilon \cdot i = \exp[\overline{\Omega} \cdot (-\zeta_{eq} \pm i\sqrt{1 - \zeta_{eq}^2})] \tag{4.1}$$

where σ and ε are the real and imaginary components; and i is the imaginary unit defined as $i = \sqrt{-1}$. The apparent frequency $\overline{\Omega}$ and equivalent damping ratio ζ_{eq} are defined as

$$\overline{\Omega} = \tan^{-1}(\varepsilon/\sigma)/\sqrt{1 - \zeta_{eq}^2} \tag{4.2a}$$

$$\zeta_{eq} = -\ln(\sigma^2 + \varepsilon^2)/(2\overline{\Omega}) \tag{4.2b}$$

Two criteria are used in the present study to evaluate the effect of estimated structural stiffness on the explicit CR algorithm, i.e., period elongation and numerical damping, which are defined as

$$PE = (\overline{T} - T_n)/T_n \tag{4.3a}$$

$$ND = \zeta_{eq} - \zeta_n \tag{4.3b}$$

where $\overline{T}$ is the period from the calculated response defined as $\overline{T} = 2\pi/(\overline{\Omega}/\Delta t)$. The period elongation evaluate the period distortion due to the estimated structural stiffness, while the numerical damping assesses the damping introduced to the SDOF structure by the CR algorithm through the estimated structural stiffness.
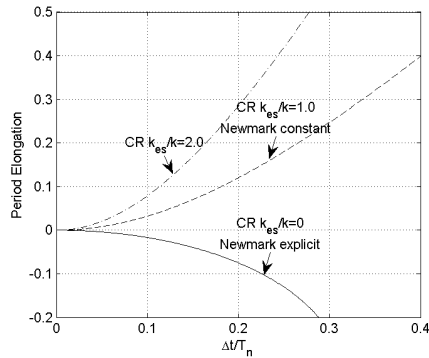

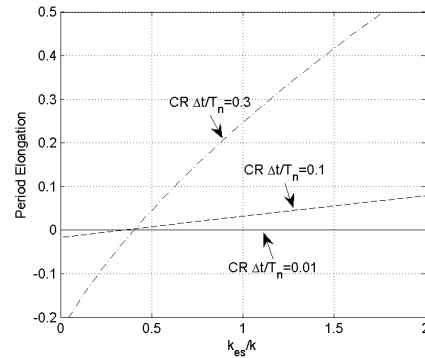**Figure 4.1.** Period elongation of CR algorithm with different estimated stiffness

Figure 4.2. Period elongation of CR algorithm with different estimated stiffness

The period elongation of the explicit CR algorithm with estimated stiffness is presented in Fig. 4.1 for different values of k_{es}/k with zero inherent viscous damping. Also presented in Fig. 4.1 is the period elongation of the Newmark explicit method and the Newmark method with constant average acceleration, which are designated as Newmark explicit and Newmark constant, respectively. With different values of k_{es}/k equal to 0.0, 1.0 and 2.0, the CR algorithm shows different period distortion property. For the cases of k_{es}/k equal to 1.0 and 2.0, the algorithm introduces period elongation (i.e., positive values of PE), while for the case k_{es}/k equal to 1.0, the CR algorithm introduces the same

period shortening as the Newmark explicit method. When the structural stiffness is underestimated, i.e., $0.0 \leq k_{es}/k \leq 1.0$, the period elongation of the CR algorithm falls between that of the Newmark explicit method and the Newmark method with constant average acceleration. When an overestimated structural stiffness is used, the CR algorithm will introduce larger period elongation than the Newmark method with constant average acceleration for the same value of $\Delta t/T_n$.

Fig. 4.2 presents the variation of period elongation for the CR algorithm with respect to k_{es}/k for different values of $\Delta t/T_n$=0.01, 0.1 and 0.3. It can be observed that the period elongation property of the CR algorithm increases almost linearly with respect to the ratio of k_{es}/k for all different values $\Delta t/T_n$. For a small value of $\Delta t/T_n$ (i.e., $\Delta t/T_n$=0.01), the CR algorithm has almost zero period distortion for k_{es}/k between zero and 2.0. When the value of $\Delta t/T_n$ increases to 0.1 and 0.3, the algorithm has period shortening for small values of k_{es}/k and period elongation for large values of k_{es}/k. It can also be observed that when the ratio between the integration time step and the natural period of the SDOF structure is smaller than or equal to 0.1, the period elongation is less than 0.1 for the range of k_{es}/k between zero and 2.0.
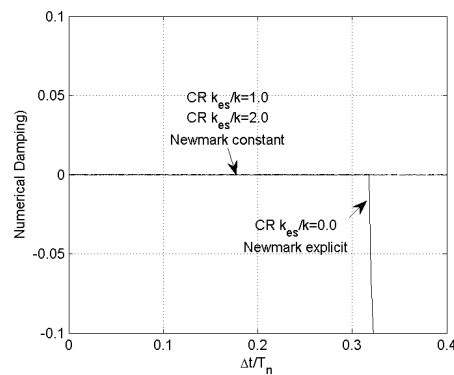

Figure 4.3. Numerical damping of CR algorithm with different estimated stiffness

The numerical damping of the CR algorithm is presented in Fig. 4.3 for different values of k_{es}/k with ζ_n=0. The numerical damping of Newmark explicit method and the Newmark method with constant average acceleration are also presented in Fig. 4.3 for the purpose of comparison. It can be observed that the CR algorithm starts to introduce negative numerical damping around $\Delta t/T_n$=0.318 (i.e., $\omega_n \Delta t$=2.0) for k_{es}/k equal to zero, indicating that the algorithm becomes unstable. This is consistent with the stability analysis Eq. (3.5b). For the other cases in Fig. 4.3, i.e., k_{es}/k=1.0 and 2.0, the explicit CR algorithm is shown to have zero numerical damping.

5. NUMERICAL SIMULATION USING CR INTEGRATION ALGORITHM

Numerical simulations of both linear and nonlinear SDOF structures are presented in this section to evaluate the effect of estimated stiffness on the explicit CR integration algorithm.

5.1. Linear elastic SDOF structure

The linear elastic SDOF structure for the numerical analysis is assumed to have a lumped mass of 503.4 metric tons, a viscous damping ratio ζ of 0.02, and a natural frequency of 1.30 Hz. The N196E component of the 1994 Northridge earthquake recorded at Canoga Park is selected as the ground motion and is scaled to have a maximum ground acceleration of 0.838 m/s^2. Figs. 5.1(a) and 5.2(a) present the comparison of the structural responses calculated using the explicit CR algorithm for the linear elastic SDOF structure subjected to the selected ground motion. Different structural stiffness estimates are used for the integration parameters, including k_{es}/k=0, 1.0 and 2.0. Compared with the actual stiffness, the values of k_{es}/k=0 and k_{es}/k=2.0 represent 100% under- and over- estimation, respectively, which gives a reasonable range for the estimated stiffness of the experimental structure in

the laboratory. The values of $\Delta t=10/1024$ *sec*. and $\Delta t=20/1024$ *sec*. are used for the integration time step for Figs. 5.1 and 5.2, respectively, leading to $\omega_n\Delta t=0.08$ and 0.16. Also presented in Figs. 5.1(a) and 5.2(a) is the structural response of the SDOF structure calculated Newmark method with constant acceleration, which will be referred to as *exact solution*. The linear elastic SDOF structure has a maximum displacement response of around 108.5 mm. Good agreement can be observed between the calculated structure responses from the CR algorithm and the exact solution for both cases, indicating that the explicit CR integration algorithm retains good accuracy under the selected estimates of the structural stiffness.
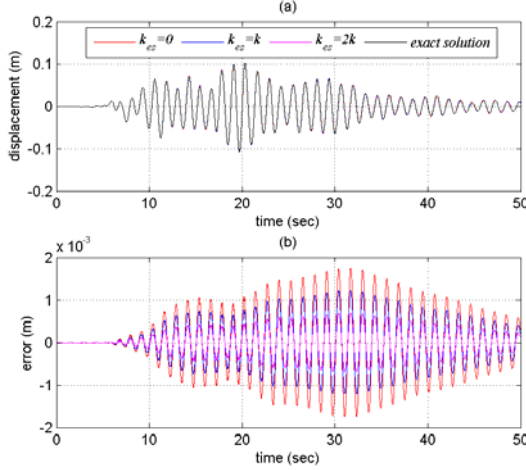

Figure 5.1. Comparison of time history analysis for linear elastic SDOF structure using CR algorithm with estimated stiffness ($\Delta t=10/1024$ *sec.*)
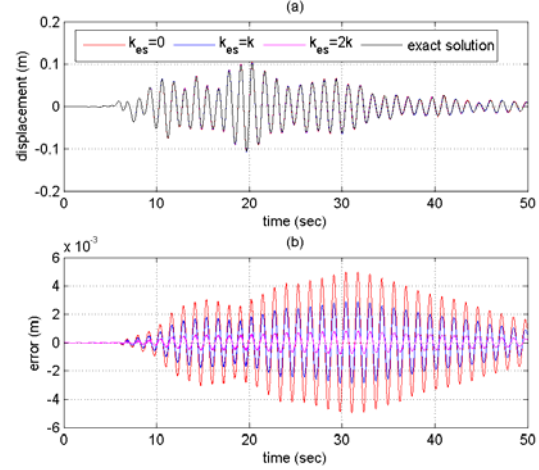
Figure 5.2. Comparison of time history analysis for linear elastic SDOF structure using CR algorithm with estimated stiffness ($\Delta t=20/1024$ *sec.*)

The differences between the calculated structural responses and the exact solution are presented in Figs. 5.1(b) and 5.2(b). A maximum error of to 1.8 mm, 1.2 mm and 0.7 mm occurs in Fig. 5.1(b) for the cases of $k_{es}/k=0$, $k_{es}/k=2.0$ and $k_{es}/k=1.0$, respectively, which correspond to 1.7%, 1.1% and 0.6% of the maximum displacement response of the SDOF structure. When a larger time step is used, i.e., $\Delta t=20/1024$ *sec.,* the maximum error for the calculated structural response in Fig. 5.2(b) is equal to 5.0 mm, 3.0 mm and 1.0 mm, for the cases of $k_{es}/k=0$, $k_{es}/k=2.0$ and $k_{es}/k=1.0$, respectively, and corresponds to 4.6%, 2.8% and 0.9% of the maximum displacement response of the SDOF structure. This again demonstrates that the explicit CR integration algorithm has good accuracy for the linear elastic SDOF structure for a range of ratio k_{es}/k between 0.0 and 2.0.

5.2. Nonlinear SDOF Structure

The nonlinear SDOF structure is assumed to have the same properties of mass, inherent viscous damping and linear elastic stiffness as the linear elastic SDOF structure discussed above. The Bouc-Wen model [Wen 1980] is used to model the nonlinear structural behavior of the SDOF structure, of which the restoring force is defined as

$$r(t) = \eta \cdot k \cdot x(t) + (1-\eta) \cdot k \cdot x_y \cdot z(t) \tag{5.1a}$$

where x_y is the yield displacement of the SDOF structure; k is the linear elastic stiffness; η is the ratio of the post- to pre-yield stiffness; and $z(t)$ is the evolutionary parameter of the Bouc-Wen model governed by the following differential equation:

$$x_y \cdot \dot{z}(t) + \gamma \left| \dot{x}(t) \right| \cdot z(t) \cdot \left| z(t) \right|^{q-1} + \beta \cdot \dot{x}(t) \cdot \left| z(t) \right|^q - \dot{x}(t) = 0 \tag{5.2b}$$

The dimensionless parameters γ, β and q in Eq. (5.2b) control the shape of the hysteretic loop of the nonlinear SDOF structure [Wen 1980]. The values of the parameters of the Bouc-Wen model used in this paper are given in Table 3.
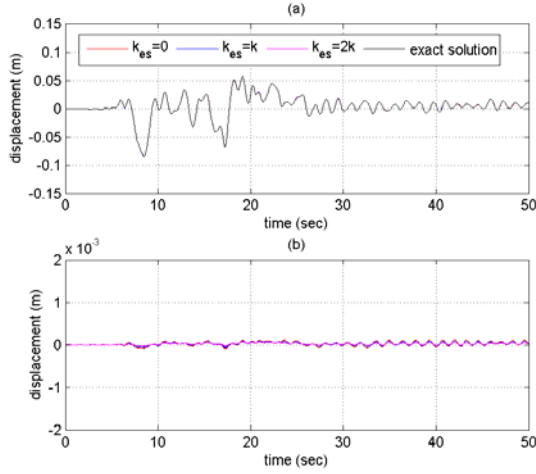

Figure 5.3. Comparison of time history analysis for nonlinear SDOF structure using CR algorithm with estimated stiffness (Δt=10/1024 *sec.*)
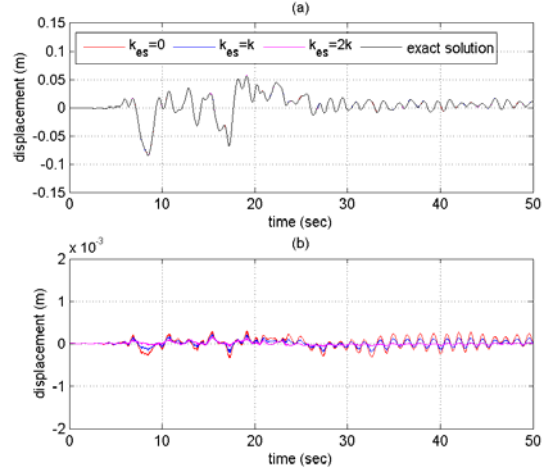
Figure 5.4. Comparison of time history analysis for nonlinear SDOF structure using CR algorithm with estimated stiffness (Δt=20/1024 *sec.*)

Table 5.1 Parameters of the Bouc-Wen Model for the Analytical Substructure

Parameter	k_a (KN/mm)	η	x_y^a (mm)	β	γ	q
Value	11.76	0.01	10	0.55	0.45	2

Figs. 5.3(a) and 5.4(a) present the comparison of the calculated structural responses of the nonlinear SDOF structure using the explicit CR algorithm with the converged solution from the Newmark method with constant average acceleration, which is referred to as *exact solution*. Different estimates of the stiffness are used to determine the integration parameters for the CR algorithm, including k_{es}/k=0, 1.0 and 2.0. Two different values, 10/1024 *sec.* and 20/1024 *sec.* are used for time step. Good agreement can again be observed between the calculated responses and the exact solution in Figs. 5.3(a) and 5.4(a). The nonlinear SDOF structure has a maximum displacement response of around 85 mm. The differences between the calculated responses and the exact solution are presented in Figs. 5.3(b) and 5.4(b). A smaller difference can be observed when compared with that in Figs. 5.3(b) and 5.4(b). The maximum error for all three cases is shown to be less than 1 mm, which is about 1.2 % of the maximum structure response. The better accuracy of the CR algorithm for the nonlinear SDOF structure with same estimated structural stiffness can be attributed to the small value of $\omega_t \Delta t$ when the structure develops nonlinear behaviour, where ω_t is the circular frequency corresponding the tangent stiffness. Figs. 5.3 and 5.4 indicate that the explicit CR algorithm again retains good accuracy for the selected nonlinear SDOF structure.

6. SUMMARY AND CONCLUSION

The effect of estimated structural stiffness on the stability and accuracy of unconditionally stable explicit CR algorithm is investigated in this paper. A root locus approach from discrete control theory is used in the stability analysis. The estimated structural stiffness is shown to affect the unconditional stability of the algorithm. For a linear elastic structure, an under-estimated stiffness (i.e., $k_{es}<k$) will decrease the stability limit, while the integration algorithms with an over-estimated stiffness (i.e., $k_{es}>k$) will help the algorithm maintain the unconditional stability. When a positive estimated stiffness is used, the CR algorithm is demonstrated to always have larger stability limit than the commonly used Newmark explicit method. The accuracy of the explicit CR algorithm under estimated structural stiffness is investigated through the poles of the discrete transfer function for linear elastic structures.

The algorithm is shown to have same period elongation as the Newmark explicit method when a zero value of the estimated stiffness is used. A period elongation is introduced for an over-estimated stiffness. When an under-estimated stiffness is used, the algorithm introduces period shortening for small values of $\omega_n \Delta t$ and period elongation for large values of $\omega_n \Delta t$. For both cases, zero numerical damping is introduced for the CR algorithm. Numerical simulations of both linear elastic and nonlinear SDOF structures are presented to evaluate the performance of the explicit CR algorithm with estimated values of structural stiffness. The CR algorithm was shown to have good accuracy when the estimated stiffness is between 0 and two times of the exact value of the linear elastic stiffness for linear structures. For nonlinear structures, a better accuracy is observed for the CR algorithm when estimated stiffness is used for the experimental specimen. The CR algorithm therefore provides a viable choice for real-time testing in earthquake engineering research

REFERENCES

Chen, C. and Ricles, J.M. (2008a). "Development of Direct Integration Algorithms for Structural Dynamics Using Discrete Control Theory." *Journal of Engineering Mechanics,* 134:8, 676-683.

Chen, C. and Ricles, J.M. (2008b). "Stability Analysis of Direct Integration Algorithms Applied to Nonlinear Structural Dynamics." *Journal of Engineering Mechanics*, 134:9, 703-711.

Chen, C., Ricles, J.M., Marullo, T. and Mercan, O. (2009). "Real-Time Hybrid Testing Using the Unconditionally Stable Explicit CR Integration Algorithm." *Earthquake Engineering and Structural Dynamics, 38:1, 23-44.*

Chen, C. and Ricles, J.M. (2010). "Tracking Error-Based Servo-Hydraulic Actuator Adaptive Compensation for Real-Time Hybrid Simulation," *Journal of Structural Engineering, 136:4, 432-440.*

Chen, C. and Ricles, J.M. (2011), "Analysis of Implicit HHT-α Integration Algorithm for Real-Time Pseudodynamic Testing," *Earthquake Engineering and Structural Dynamics*, 41:5, 1021–1041.

Franklin, G.F., Powell, J.D. and Naeini, A.E. (2002), *Feedback Control of Dynamic System*, 4th Edition, Prentice-Hall, New Jersey.

Lin, Y.C., Ricles, J.M. and Sause, R. (2008). "Earthquake Simulations On A Self-Centering Steel Moment Resisting Frame With Web Friction Devices." 14th World Conference on Earthquake Engineering, Beijing, China.

Nakashima, M., Kaminoso, T., Ishida M. and Kazuhiro, A. (1990). "Integration techniques for substructure online test." Proceedings, 4th U.S. National Conference of Earthquake Engineering, Palm Springs, California.

Newmark, N.M. (1959). "A Method of Computation for Structural Dynamics." *Journal of Engineering Mechanics Division*, ASCE, 85, EM3, 67-94.

Ogata, K. (1995). *Discrete-Time Control Systems*, 2nd Edition, Prentice-Hall, New Jersey.

Oliva, M., Gavrilovic, P. and Clough, R.W. (1990), "Seismic testing of large panel precast walls: Comparison of pseudostatic and shaking table tests," *Earthquake Engineering and Structural Dynamics*, 19:6, 859-875.

Roke, D., Sause, R., Ricles, J.M. and Gonner, N. (2008). "Design concepts for damage-free seismic-resistant self-centering steel concentrically-braced frames." 14th World Conference on Earthquake Engineering, Beijing, China.

Seo, C.Y., Lin, Y.C., Sause, R. and Ricles, J.M. (2009). "Development of analytical models for 0.6 scale self-centering MRF with beam web friction devices." Behavior of Steel Structure in Seismic Areas (STESSA), Philadelphia, PA.

Shing, P.B. (2002), "Development of high-speed on-line substructuring testing system at the University of Colorado," *CASCADE Technical Workshop,* Oxford, UK.

Shing, P.B. and Vannan, M.T. (1991), "Implicit time integration for pseudodynamic tests: Convergence and energy dissipation," *Earthquake Engineering and Structural Dynamics*, 20:9, 809-819.

Wen, Y.K. (1980), "Equivalent linearization for hysteretic systems under random excitation," *Journal of Applied Mechanics*, Transaction of ASME, 47:150-154.

Yang, G.Q., Spencer, B.F., Carlson, J.D. and Sain, M.K. (2002). "Large-scale MR fluid dampers: modeling and dynamic performance considerations." *Engineering Structures*, 24:3, 309-323.

Zhang, X.F. and Ricles, J.M. (2006), "Experimental evaluation of reduced beam section connections to deep columns," *Journal of Structural Engineering*, 132:3, 346-357.